ELSEVIER

Journal of Nuclear Materials 241-243 (1997) 1031-1035

journal of nuclear materials

Laboratory experiments on hydrogen and impurity behaviors in lithium-deposited environment

H. Toyoda *, M. Watanabe, H. Sugai

Department of Electrical Engineering, Nagoya University, Furo-cho, Chikusa-ku, Nagoya 464-01, Japan

Abstract

Wall conditioning with deposition of thin lithium layers gives rise to low hydrogen recycling and reduction in oxygen and carbon impurities. To understand such effects, small-scale laboratory experiments are carried out mainly focusing on the chemical state of hydrogen involved in the lithium layer. First, measurements of the methane yield from graphite walls in a hydrogen glow discharge reveal that the lithium deposition leads to ~ 25% reduction of chemical sputtering. Second, thermal desorption of hydrogen molecules from the lithium layer suggests existence of different states of hydrogen: one is weakly bound hydrogen which is released from the lithium layer at $T \sim 200°C$, and the other is attributed to lithium hydride which decomposes for $T > 400°C$. Finally, a new wall conditioning based on a lithium borohydride ($LiBH_4$) discharge is demonstrated, which enables co-deposition of lithium and boron.

Keywords: Wall conditioning; Wall coating; Low Z wall material; Wall pumping; Plasma–wall interaction simulator

1. Introduction

There has been a growing interest in wall conditioning with lithium layer deposition since the first laboratory experiment [1] and lithium pellet injection on TFTR [2]. To date, the lithium conditioning has been done in several devices; TFTR [2-5], TdeV [6], JIPP-TIIU [7], DIII-D [8] and Heliotron-E [9]. In most cases, the main effect has been substantial decrease in oxygen and carbon impurities along with low hydrogen recycling.

In addition, small-scale laboratory studies [7,10] revealed various chemical activities of the lithium layer, supporting the observations in fusion devices. First, the lithium layer at room temperature getters most of residual gases such as H_2O, O_2, CO and CH_4. In the case of O_2, the maximum oxygen uptake is about one half the number of lithium atoms deposited on the wall, thus suggesting formation of Li_2O. Second, the deposition of a thin lithium layer on graphite walls dramatically suppresses the release of CO molecules in interaction with plasmas containing oxygen. However, more investigations are needed on physical sputtering as well as hydrogen-induced chemical sputtering of graphite. Third, an exposure of the lithium surface to a hydrogen plasma leads to an enormous uptake of hydrogen in the lithium layer. The hydrogen uptake ceases when the lithium layer is saturated with hydrogen at the atomic ratio $H/Li \sim 1$, suggesting lithium hydride (LiH) formation. Finally, thermal desorption of hydrogen molecules from the lithium layer saturated with hydrogen is observed at 200°C which is much lower than the melting point (680°C) of LiH. Thus, there remains a question about the chemical state of hydrogen atoms in the lithium layer, although a chemical shift of Li ls in XPS analysis suggests existence of Li–H bond..

To make the lithium conditioning effects clear, further clear-cut studies on plasma–lithium interactions are required. In this paper, we describe basic experiments on the chemical state of hydrogen in lithium and on chemical sputtering of lithium-covered graphite. The former is significant from a hydrogen inventory control point of view. Finally, we report preliminary experiments on a new con-

---

* Corresponding author. Fax: +81-52 789 3150; e-mail: toyota@nuee.nagoya-u.ac.jp.

PII S0022-3115(96)00654-X

ditioning technique with Li/B co-deposition using a lithium borohydride plasma.

2. Experimental

The basic experiment was performed in a small laboratory apparatus shown in Fig. 1. The outer stainless steel vessel of 0.3 m diameter and 0.6 m length is evacuated with a turbomolecular pump. In cases of graphite wall experiments, a sheet of graphite (Toyo Tanso, perma foil PF-UHPL, 0.38 mm thick) is attached onto the inner stainless steel vessel of 0.27 m diameter and 0.45 m length, as shown in Fig. 1. Using a resistive heating system, the temperature of the graphite wall is maintained at a constant value in the range 30–400°C.

Lithium is deposited onto walls in vacuum by heating a lithium-containing oven up to 450°C. A deposition monitor based on quartz crystal oscillation is used to measure the lithium deposition rate in situ. After lithium deposition, a dc glow discharge is turned on (voltage ~ 300 V, current ~ 0.3 A, current density on the wall ~ 60 $\mu A/cm^2$) by applying a dc voltage between a stainless steel mesh anode (2 cm × 1 cm) and the grounded vessel (cathode). The ion energy bombarding the wall is ~ 300 eV as given by the cathode fall. Hydrogen absorption into lithium layers and methane desorption from graphite walls is monitored by a quadrupole mass analyzer (QMA).

Thermal desorption experiments are carried out by inserting a test wall which is a thin nickel foil (8 cm × 2 cm, 0.04 mm thick) enabling a rapid heating with a dc current. After exposing the lithium-deposited wall to a hydrogen glow for ~ 10 min, hydrogen molecules are released from the lithium layer by heating the test wall in vacuum from 30 to 800°C at a typical rate of 4°C/s. The time evolution of hydrogen pressure is monitored by the QMA.

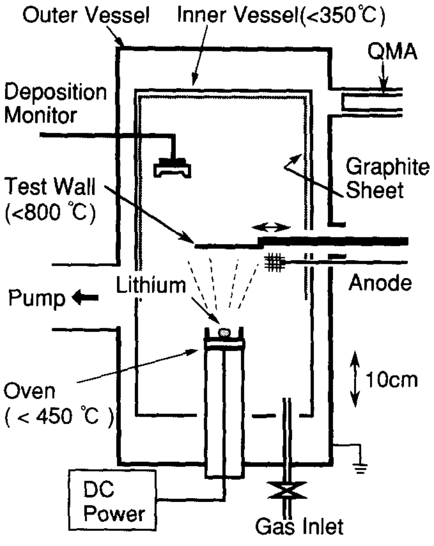

Fig. 1. Schematic of experimental apparatus for lithium deposition, plasma–lithium interactions and thermal desorption studies.

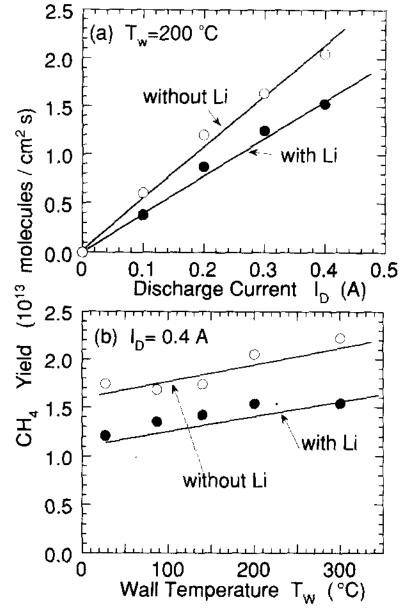

Fig. 2. Methane yield from graphite walls with/without lithium deposition, for (a) constant wall temperature $T_w = 200°C$ and (b) the constant discharge current $I_D = 0.4$ A.

3. Chemical sputtering of lithium-deposited graphite

In connection with carbon impurity reduction by lithium pellet injection on TFTR [2–5], chemical sputtering of graphite was investigated here. The graphite sheet wall shown in Fig. 1 is covered with a 50–200 nm thick lithium layer by vacuum evaporation of lithium from the oven. After the lithium deposition at room temperature, the graphite wall is heated and kept at a constant wall temperature T_w = 30–300°C. Then, the hydrogen glow discharge is turned on to measure the methane yield induced by the plasma–graphite interaction.

Fig. 2 shows the methane yield measured for the different values of the discharge current I_D and the wall temperature T_w, comparing the data with and without lithium deposition. As seen in Fig. 2(a), the methane linearly increases with the current I_D, suggesting a linear increase in the hydrogen ion and atom fluxes onto the wall with almost constant discharge voltage, and constant ion bombarding energy (~ 300 eV). On the other hand, the methane yield weakly increases with the wall temperature in Fig. 2(b) as the present temperature is below a regime of high chemical sputtering of graphite (T_w = 400–700°C).

When the lithium layer is deposited, the methane yield is reduced by ~ 25% compared with the case of bare graphite surfaces. If the graphite surface could be completely covered with lithium layers, then, no methane would be released. However, the graphite sheet surface is so rough (roughness scale > 10 μm) that lithium evaporation cannot fully mask the graphite surfaces, leaving bare shadow regions including porous and microchannel regions. This might be a reason for the relatively small influence of Li deposition observed in the present experiment.

In fusion devices, carbon impurities are created not only from chemical sputtering but also from physical sputtering. Both types of graphite sputtering will be reduced by lithium deposition according to several mechanisms; (1) direct masking of graphite surfaces with lithium layer, (2) formation of Li-C chemical bonding at the interface, and (3) reduction of hydrogen flux onto walls as a consequence of low hydrogen recycling induced by lithium deposition.

4. Formation of LiH and thermal desorption of H_2

Thermal desorption of hydrogen molecules from the lithium layer which had been exposed to hydrogen glow was measured to get information on chemical state of hydrogen. First of all, the inner vessel shown in Fig. 1 was removed inserting the test wall. A 40-100 nm thick layer of lithium is deposited in vacuum onto the test wall except the outer vessel wall, and then without opening the vessel it is exposed to a hydrogen glow plasma (produced in the same way described in Section 3) for 10 min at room temperature until it is fully saturated with hydrogen uptake. After these preparations, the test wall is rapidly heated in vacuum from 30 to 800°C at a typical ramp rate of 4°C/s, while the temperature dependent thermal desorption of H_2 molecules is measured by the QMA.

Fig. 3 shows examples of thermal desorption spectra (TDS). The curve labeled 'A' shows a clear peak at $T \sim 200°C$ just around the melting point (179°C) of lithium. The time integration of hydrogen release rate gives the total hydrogen inventory, which was the same order of magnitude as the hydrogen uptake estimated from the pressure decrease during the hydrogen glow discharge. Thus, most of hydrogen atoms contained in the lithium layer are easily desorbed at relatively low temperatures.

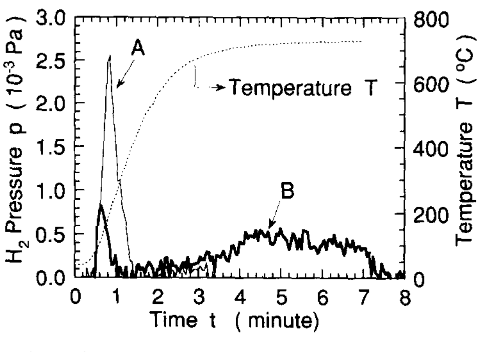

Fig. 3. Thermal desorption of hydrogen molecule from lithium-deposited wall. The solid lines A and B indicate hydrogen pressures and the dashed line the test wall temperature.

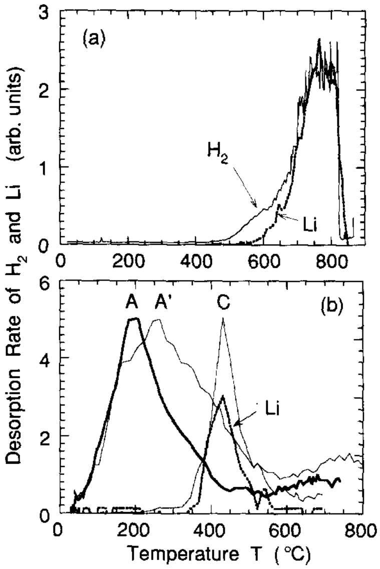

Fig. 4. Thermal desorption rate of H_2 molecule and Li atom from (a) lithium hydride powder and (b) lithium-deposited walls after exposure to hydrogen glow at different base pressures.

However, the TDS seems to depend on the experimental history and circumstances. For instance, the curve 'B' in Fig. 3 was obtained as follows. The test wall with the lithium layer containing H_2 is heated at a slow ramp rate (0.25°C/s) up to 300°C, kept there for 60 min, again exposed to the hydrogen glow at room temperature for 10 min, and finally heated at a fast ramp rate to 700°C as shown in Fig. 3. In this case, hydrogen molecules are released not only at low temperatures (< 200°C) but also at high temperatures around the melting point (680°C) of lithium hydride.

To measure the thermal properties of LiH, commercially available lithium hydride powder was put on the test wall and heated in vacuum. Hydrogen molecules and lithium atoms released from the LiH powder were measured by the QMA and the deposition monitor, respectively, as shown in Fig. 4(a). Since H_2 and Li evolve in the same manner, it is concluded that thermal decomposition of lithium hydride, $2LiH \rightarrow 2Li + H_2$, takes place for $T > 400°C$ and eventually none of the original lithium remains on the wall. Thus, the second peak of the curve B in Fig. 3 at $T \sim 700°C$ is interpreted as the thermal decomposition of LiH and the first peak for $T < 200°C$ will be discussed later.

The curve A in Fig. 3 is replotted as a function of the temperature as shown in Fig. 4(b), together with other TDS curves labeled A′ and C. Here the base pressure in the TDS experiments is always lower than 2.7×10^{-4} Pa. In the hydrogen glow discharge, however, the pumping speed was decreased from 50 l/s to 5 l/s in order to maximize the hydrogen pressure drop induced by lithium-plasma interaction. In this case, the base pressure evolves to 4×10^{-3} Pa for the curve A and 2.7×10^{-3} Pa for the curve A′. On the other hand, the curve C was taken for much lower base pressure, 4×10^{-4} Pa, and the hydrogen release does not occur at $T \sim 200$°C but sharply increases for $T > 400$°C. It should be noted here that H_2 and Li evolution occurs simultaneously and finally cease as a consequence of the complete evaporation of lithium. The measured release rate (0.1 nm/s) of Li at 450°C is much smaller than that of the evaporation rate (70 nm/s) of metallic lithium, suggesting that the release rate is probably determined by the decomposition rate of LiH. The base pressure for the curve B (see Fig. 3) is lower than that for the curve A since the already deposited lithium layer works as a getter pump.

These observations suggest that high quality lithium hydride can be formed in clean conditions. On the other hand, high base pressures with a main residual component of water lead to low quality LiH films, which contain loosely bound hydrogen atoms and a small amount of oxygen atoms, thus releasing hydrogen molecules at lower temperatures. We have eliminated the possibility that lithium hydroxide (LiOH) was formed, since the TDS of commercially available LiOH showed H_2O release but not H_2 at $T > 450$°C by the decomposition reaction, $2LiOH \rightarrow Li_2O + H_2O$.

5. Li/B co-deposition by a lithium borohydride discharge

A preliminary experiment of lithium/boron co-deposition for wall conditioning was performed in another device of 0.2 m diam. and 0.49 m length, which is bakeable to 400°C and has been previously used for boronization studies [11]. The source substance used is commercially available powder of lithium borohydride ($LiBH_4$) which melts at 268°C and decomposes at 380°C. This compound may be formed in fusion devices where a lithium layer is deposited on boronized walls. Heating the lithium borohydride powder in vacuum gives rise to evaporation of $LiBH_4$ molecules. However, these molecules condenses on the metal vessel wall when the wall temperature is lower than 200°C. To prevent such condensation, the entire vessel is kept at ~ 350°C and one gram of lithium borohydride powder is directly scattered on the bottom lid.

A dc glow discharge (170 V, 0.3 A) in helium at a pressure of 18 Pa was a pink in color due to optical emission from lithium atoms under $LiBH_4$ evaporation in the hot wall vessel. After seven hours, the discharge color changed to pale green as observed in ordinary helium discharges, thus indicating the end of lithium borohydride evaporation. Fig. 5 shows the representative spectra of optical emission observed during the discharge. In addition to HeI emission, the discharge decomposition of $LiBH_4$ molecule gives the intense emission lines from Li atom, BH radical, and H atom. The atomic composition of 1 μm thick film deposited on a silicon substrate was ex situ measured by Auger electron spectroscopy which clearly showed peaks of Li and B atoms along with O and C impurities. The atomic ratio Li/B is expected to be close to unity since the plasma decomposition of $LiBH_4$ gives no detectable volatile gas except for H_2. It is notable that the films are electrically conductive although the conductivity is much lower than the one of lithium.

After deposition of Li/B layer onto the vessel wall, a short glow discharge (28 s, 300 V, 0.3 A) in 40 Pa hydrogen was turned on to investigate an interaction with hydrogen plasma. Fig. 6(a) shows a temporal variation of hydrogen pressure caused by the hydrogen discharge with the wall temperature kept at $T_w = 350$°C. Time integration of the measured pressure drop $\Delta p(t)$ from $t = 0$ to $t = 28$ s with a pumping speed taken into account gives a total amount of hydrogen uptake into the Li/B layer to be 6.5×10^{20} atoms/m^2. This amount is larger than the value (2.0×10^{20} atoms/m^2) obtained in diborane-based boronization at $T_w = 300$°C [11], while a pure lithium layer can absorb much more hydrogen atoms depending on the layer thickness as reported previously [7].

Subsequent to the hydrogen discharge experiment, chemical reactions of Li/B layer with oxygen at T_w =

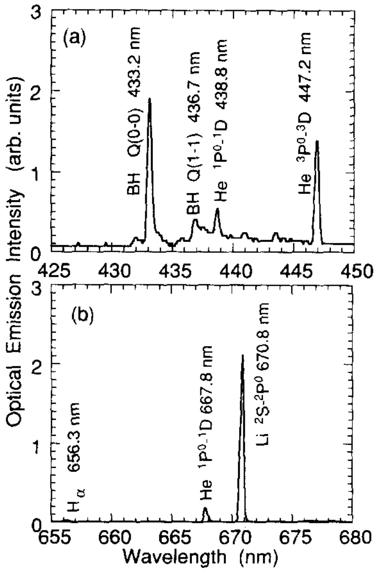

Fig. 5. Examples of optical emission spectra observed in $LiBH_4$/He discharge.

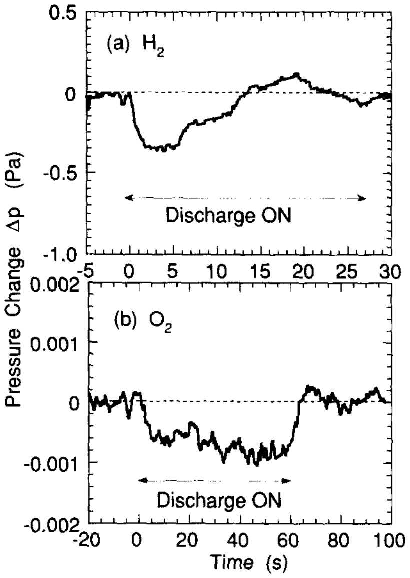

Fig. 6. (a) Hydrogen pressure change induced by a 28 s pulsed discharge in 40 Pa hydrogen. (b) Oxygen partial pressure changes induced by a 60 s pulsed discharge in a mixture gas 0.04 Pa O_2 +40 Pa He.

350°C were investigated using a glow discharge (200 V, 0.3 A) in an oxygen mixture gas (0.04 Pa O_2 + 40 Pa He). Fig. 6(b) shows the discharge induced change in O_2 pressure. The oxygen uptake is evaluated by integrating $\Delta p(t)$ from $t = 0$ to 60 s, which is 2.6×10^{19} atoms/m^2 and an order of magnitude smaller than the conventional boronization [11]. Such weak oxygen gettering could come from pre-oxidation: when oxygen gas is introduced into the vessel, oxygen molecules may react and oxidize the Li/B layer before a discharge ignition, as previously observed in the lithium layer [7]. In the present experiment, however, pre-oxidation was dismissed because a mass flow controller was not used for oxygen gas injection.

6. Conclusion

The basic laboratory studies were made to elucidate the mechanisms of fuel and impurity control by lithium wall conditioning. First, the reduction in the carbon impurity observed in fusion devices is supported by measurements of the methane yield from graphite in a hydrogen glow discharge. That is, the chemical sputtering is reduced by ~ 25% with lithium deposition onto graphite surfaces and a few additional factors important for carbon impurity suppression were pointed out.

Exposure of a lithium layer to hydrogen plasma gives rise to hydrogen uptake up to a saturation level of H:Li = 1:1, as reported previously. The chemical state of hydrogen involved in the lithium layer was evaluated in thermal desorption studies. As a consequence, the following two cases were found. Interactions with a clean hydrogen plasma eventually convert a lithium layer to a lithium hydride layer which is thermally decomposed at temperatures higher than 400°C. On the other hand, hydrogen plasma interactions in the presence of trace impurities such as oxygen give rise to weakly bound hydrogen which is easily released from the lithium layer at low temperatures (~ 200°C). Such low temperature desorption of hydrogen molecules may be used for reducing hydrogen inventory by wall heating.

To date, thin lithium layers have been deposited solely with use of solid lithium. A new possibility of using lithium borohydride ($LiBH_4$) was demonstrated for the first time in this paper. A glow discharge in a $LiBH_4$ vapor mixed with helium leads to co-deposition of lithium and boron on hot walls. These preliminary experiments showed the hydrogen uptake and the oxygen gettering effects by Li/B layers.

Acknowledgements

The authors would like to thank Dr. F.L. Tabares, CIEMAT, Spain for his proposal to use lithium borohydride. This work was supported by a Grant-in-Aid for Scientific Research from the Ministry of Education, Science, Sports and Culture in Japan.

References

[1] T. Isozumi, S. Yoshida and H. Sugai, Kaku Yugo Kenkyu 60 (1988) 304.
[2] J.A. Snipes et al., J. Nucl. Mater. 196-198 (1992) 686.
[3] D.K. Owens et al., J. Nucl. Mater. 220-222 (1995) 62.
[4] D.K. Mansfield et al., Phys. Plasmas 3 (1996) 1892.
[5] K.M. McGuire et al., Phys. Plasmas 2 (1995) 2176.
[6] B. Terreault et al., J. Nucl. Mater. 220-222 (1995) 790.
[7] H. Sugai, H. Toyoda, K. Nakamura, K. Furuta, M. Ohori, K. Toi, S. Hirokura and K. Sato, J. Nucl. Mater. 220-222 (1995) 254-258.
[8] G.L. Jackson, these Proceedings, p. 655.
[9] K. Kondo et al., presented in Annu. Meet. of the Japan Soc. of Plasma Sci. and Fusion Research (Kyoto, March 1996).
[10] H. Sugai, M. Ohori and H. Toyoda, Vacuum 47 (1996) 981.
[11] M. Yamage, T. Ejima, M. Saidoh, N. Ogiwara and H. Sugai, Jpn. J. Appl. Phys. 32 (1993) 3968.